China Ocean Eng., 2022, Vol. 36, No. 4, P. 565–574
DOI: https://doi.org/10.1007/s13344-022-0049-0, ISSN 0890-5487
http://www.chinaoceanengin.cn/ E-mail: coe@nhri.cn

Prediction of Collapse Pressure of Submarine Pipelines in A Wide Range of Diameter–Thickness Ratio

XU Wan-hai[a, *], PANG Tao[a], YAN Shu-ming[b], ZHAI Li-bin[b], KANG You-wei[b], ZHANG Shu-hai[b]

[a] State Key Laboratory of Hydraulic Engineering Simulation and Safety, Tianjin University, Tianjin 300072, China

[b] China Petroleum Pipeline Engineering Corporation, Langfang 065000, China

Received November 24, 2021; revised March 28, 2022; accepted May 20, 2022

Abstract

Submarine pipelines play an important role in offshore oil and gas development. A touchy issue in pipeline design and application is how to avoid the local collapse of pipelines under external pressure. The pipe diameter-thickness ratio D/t is one of the key factors that determine the local critical collapse pressure of the submarine pipelines. Based on the pipeline collapse experiment and finite element simulation, this paper explores the pressure-bearing capacity of the pipeline under external pressure in a wide range of diameter-thickness ratio D/t. Some interesting and important phenomena have been observed and discussed. In the range of $16<D/t<80$, both DNV specification and finite element simulation can predict the collapse pressure of pipeline quite well; in the range of $10<D/t<16$, the DNV specification is conservative compared with the experimental results, while the finite element simulation results are slightly larger than the experimental results. Further parameter analysis shows that compared with thin-walled pipes, improving the material grade of thick-walled pipes has higher benefits, and for thin-walled pipes, the ovality f_0 should be controlled even more. In addition, combining the results of finite element simulation and model experiment, an empirical formula of critical collapse pressure for thick-walled pipelines is proposed, which is used to correct the error of DNV specification in the range of $10<D/t<16$.

Key words: collapse pressure, submarine pipelines, diameter-thickness ratio, DNV specification, finite element simulation

Citation: Xu, W. H., Pang, T., Yan, S. M., Zhai, L. B., Kang, Y. W., Zhang, S. H., 2022. Prediction of collapse pressure of submarine pipelines in a wide range of diameter−thickness ratio. China Ocean Eng., 36(4): 565–574, doi: https://doi.org/10.1007/s13344-022-0049-0

1 Introduction

Submarine pipelines are generally considered to be the fastest and most economical method for long-distance transportation of oil and natural gas and have been widely used in offshore engineering applications. In recent years, with the diversified development of engineering requirements, submarine pipelines have been facing new challenges in practical engineering situations. On the one hand, with the increase in energy demand, oil and gas projects are moving toward the deep sea, which promotes the application of thick-walled pipelines (DNV, 2014). The bearing capacity of thick-walled pipelines under huge hydrostatic pressure in the deep sea has attracted more and more attention. On the other hand, thin-walled pipelines with large-diameter are widely used in oil transportation and sewage discharge under the shallow sea condition. How to ensure the stability of thin-walled structures has become a problem that needs to be solved. Thick-walled pipes and thin-walled pipes are very different in pressure-bearing capacity, the former needs to withstand huge hydrostatic pressure, while the latter has a relatively fragile structure. Therefore, local buckling becomes the main failure mode of both thick-walled pipes and thin-walled pipes. The maximum external pressure that the pipeline can withstand without internal pressure is called the critical collapse pressure P_{co}. When the external pressure exceeds P_{co}, the local defect section of the pipeline changes from a circular shape to an ellipse under the action of the external pressure until it is squashed, that is, local buckling occurs. Local buckling will further spread along the pipeline, leading to large-scale failure of the pipeline, and may even cause serious oil and gas leakage and environmental pollution problems.

Three local buckling modes of the pipeline are external overpressure failure, buckling expansion and combined load

Foundation item: This work was financially supported by the National Natural Science Foundation of China (Grant Nos. U2106223 and 51979193) and the Major Consulting Project of Academy-Local Cooperation of Chinese Academy of Engineering (Grant No. 2021DFZD2).
*Corresponding author. E-mail: xuwanhai@tju.edu.cn

failure (Bastola et al., 2014), of which external overpressure failure is the basis of the latter two modes. Accurately predicting the critical collapse pressure (P_{co}) has become the key to avoid the local buckling of the pipeline under external pressure. As one of the important issues that need to be considered in the design of submarine pipelines, the collapse mechanism of the pipeline under external pressure and the prediction of the collapse pressure P_{co} have caused extensive research works by researchers. Early studies generally believed that the pipe diameter-thickness ratio D/t, material grade and cross-sectional defects (local ovality f_0, etc.) were the main factors affecting pipeline collapse pressure. Many researchers tried to give expressions containing the above factors to solve the collapse pressure of the pipeline, among which the representative is Timoshenko's equation on the elastic collapse of the ideal ring (Timoshenko and Gere, 1961). Based on the ideal elastoplastic assumption, Haagsma and Schaap (1981) introduced the plastic hinge judgment condition and gave the solution equation of the pipeline collapse pressure, which was subsequently adopted by Det Norske Veritas (2013). The rest of the solution methods also include Langner and Ayers (1985) equation, Shell's (1975) and Murphey and Langner (1985) equations, and American Petroleum Institute (1999) formula, etc. Among the above-mentioned classic formulas for solving pipeline collapse pressure, the DNV formula is one of the most famous and widely used methods. The main solving equations are as follows:

$$P_e - P_{min} \leqslant \frac{P_{co}(t_2)}{\gamma_m \gamma_{SC}}; \tag{1}$$

$$(P_{co} - P_{el}) \cdot \left(P_{co}^2 - P_p^2\right) = P_{co} P_{el} P_p f_0 \frac{D}{t}; \tag{2}$$

$$P_{el} = \frac{2E}{1-\nu^2}\left(\frac{t}{D}\right)^3; \tag{3}$$

$$P_p = 2 f_y \alpha_{fab} \frac{t}{D}; \tag{4}$$

$$f_0 = \frac{D_{max} - D_{min}}{D}, \tag{5}$$

where P_e and P_{min} are the external hydrostatic pressure and the minimum internal pressure of the pipe, respectively; P_{el} is the elastic collapse pressure; P_p is the plastic collapse pressure; $f_0 \approx 2\Delta_0$ is the initial ovality; f_y is the yield stress of the material, and α_{fab} is the manufacturing factor.

However, the DNV specification initially limited the scope of application of the formula to $15<D/t<45$. In the face of increasingly diversified demands, especially the engineering use of deep-sea thick-walled pipes and shallow-sea ultra-thin-walled pipes, the formula has gradually shown its limitation. Palmer and King (2008) pointed out that the DNV formula is conservative in predicting the collapse pressure of thick-walled pipelines, and as D/t decreases, this deviation becomes larger. Most of the latest researches focus on the collapse of thick-walled pipes. For example, Yu et al. (2019) proposed a new numerical solution model for the collapse pressure of thick-walled pipelines based on the hypothesis of shear deformation and thick-stretched large deformation and used the experimental results of the thick-walled pipeline model to verify the correctness of the numerical model. In addition, with the development of computer technology, more research based on finite element simulation has emerged. Guarracino et al. (2011) related a large number of experimental data and finite element models and proposed an analytical expression for pipeline collapse pressure. He et al. (2014) analyzed a large number of finite element simulation results and gave a fitting formula suitable for the range of $12.5<D/t<30$. In addition to the above-mentioned D/t, ovality, and steel grade, the formula also takes into account the anisotropy of the material. Zhang and Pan (2020) continued to analyze the influence of pipeline eccentricity on the collapse pressure and gave the corresponding analytical formula based on the research work of He et al. (2014). More researches (Kyriakides and Babcock, 1981; Dyau and Kyriakides, 1993; Corradi et al., 2005; Dvorkin and Toscano, 2013) also considered the influence of material hardening coefficient, anisotropy, and residual stress on pipeline collapse pressure. However, from an engineering point of view, for the reasonable and actual eccentricity and residual stress in the manufacturing process, these factors themselves have little effect on the collapse pressure (Fallqvist, 2009; Kara et al., 2010; Mantovano et al., 2011; Bastola et al., 2014). The ratio of the outer diameter of the pipe to the wall thickness D/t is still one of the decisive factors that determine the ability of the pipe to resist collapse.

Although the latest DNV specification (DNVGL, 2017) extends the applicable range of the equation to $15<D/t<60$, there is no unified theory and solution model for thick-walled pipes ($D/t<16$) and ultra-thin-walled pipes ($D/t>60$). These are not within the scope of application of mainstream norms, and relevant studies are still controversial in terms of applicability. Moreover, there is still a lack of effective research and related experimental data on the collapse of thick-walled and ultra-thin-walled pipelines. The applicability of the DNV formula within this range needs to be verified. Therefore, to accurately predict the critical collapse pressure P_{co} of the submarine pipeline in a wide range of diameter-thickness ratio, it is necessary to perform a complete buckling analysis of the above two types of submarine pipelines. Based on extensive finite element simulations, combined with pipeline collapse experiments, this paper focuses on exploring the external pressure bearing capacity of pipelines within two D/t ranges ($D/t<15$ and $D/t>60$). The correctness and applicability of the existing classic formula and finite element simulation are verified within the above D/t range. In addition, the conservative prediction of the DNV formula of P_{co} for thick-walled pipelines is revised, and the calculation formula of critical collapse pressure suit-

able for thick-walled pipelines is proposed.

2 Numerical simulation

2.1 Finite element model

The essence of local pipeline collapse is an instability phenomenon. The finite element simulation in this paper mainly discusses the critical buckling characteristics of the pipeline under external pressure and does not further discuss the post-buckling behavior of the pipeline. ABAQUS suggests using the Riks method to solve the critical stability problem of structures (Hibbit et al., 2014). The axial length and location of the ovality also affect the collapse pressure of the pipeline (Fan et al., 2017). The average ovality of a certain distance in the axial direction of the pipeline, also known as uniform ovality f_0 (Eq. (5)), is one of the most common initial defects of submarine pipelines. In this paper, the uniform ellipticity is selected as the inducement of local pipeline collapse in the finite element model, which makes the simulation results universally applicable. Fig. 1 shows the setting of ellipticity in the finite element model. The influence of eccentricity on pipeline collapse pressure is ignored. Based on this symmetry, a three-dimensional solid 1/4 pipe model was established in ABAQUS. The length of the model is set to 10 times the outer diameter of the pipe to eliminate potential boundary effects. Fig. 2a shows the setting of the boundary conditions of the pipeline model: the uniform load applied to the outer wall of the pipeline is used to simulate the hydrostatic pressure; corresponding symmetry constraints are set on each symmetry plane, and the end of the pipeline is hinged to better simulate the long submarine pipeline. Fig. 2b shows the meshing form of the pipeline model: for the thick-walled pipe model, six layers of meshes are divided in the thickness direction to avoid the hourglass problem that may be caused by the universal element C3D8R. The mesh of the thin-walled pipe model in the thickness direction is divided into two layers and choose the three-dimensional eight-node incompatible element C3D8I (Hibbit et al., 2006; Simo and Armero, 1992) to achieve better simulation results. Both adopt the local refinement technology of the mesh at the symmetric end of the pipeline, which improves the calculation accuracy and reduces the calculation

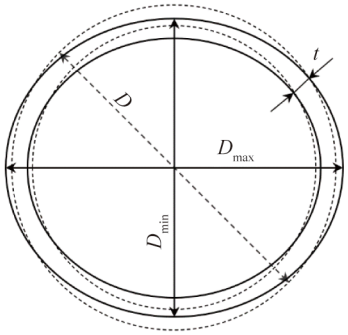

Fig. 1. Definition of initial defect f_0.

scale. The material stress-strain relationship curve of the pipe model is fitted based on the Ramberg-Osgood model (Lu et al., 2022), which is defined as follows:

$$\varepsilon = \frac{\sigma}{E}\left[1 + \frac{3}{7}\left(\frac{\sigma}{\sigma_y}\right)^{n-1}\right], \tag{6}$$

where E is the elastic modulus of the pipe, σ_y is the nominal yield limit, and n is the material hardening coefficient. All these parameters can be obtained through the material's axial tensile test.

2.2 Simulation of the pipe buckling

By taking the SS304 pipeline with D/t=25 as an example, Fig. 3a shows the buckling process of the pipeline with symmetrical elliptical defects obtained by finite element simulation. Stages 1 to 4 are the pipeline external pressure rise, local collapse, pipeline inner wall contact, and buckling propagation, which respectively correspond to the numbers 1 to 4 of the pipeline external pressure change curve in Fig. 3b. It can be seen that finite element simulation can present the phenomenon of pipe collapse under external pressure while being able to obtain detailed material stress and strain distribution. With finite element tools, subsequent calibration of experimental results and parameter study are carried out.

3 Experimental tests

To further verify the accuracy and applicability of the finite element simulation and the DNV formula in a wider range of D/t, 11 groups of buckling experimental tests,

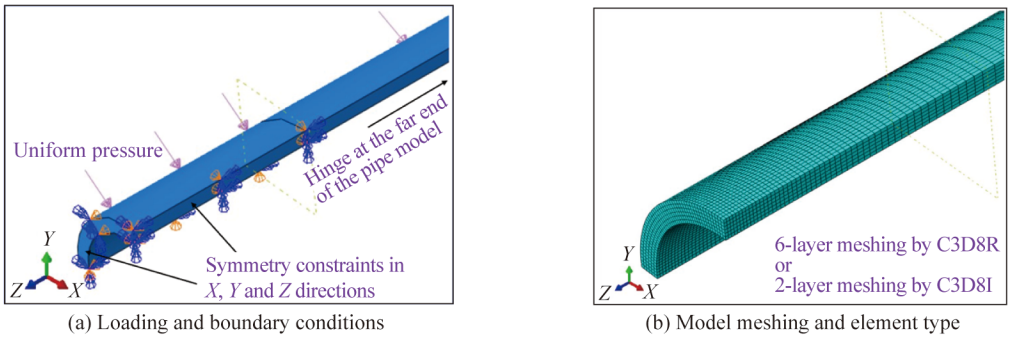

(a) Loading and boundary conditions (b) Model meshing and element type

Fig. 2. Finite element model.

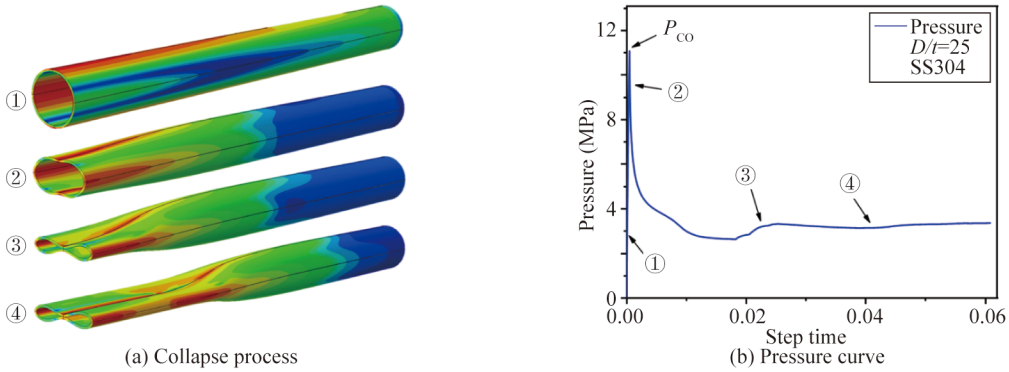

(a) Collapse process (b) Pressure curve

Fig. 3. Results of finite element simulation.

including 2 full-scale pipes and 9 reduce-scale pipes, were conducted in the general-scale hyperbaric chamber in the University of Chinese Academy of Sciences. Limited by the pressurization capacity of the experimental device, the experiment focused on the load-bearing capacity of medium-walled and ultra-thin-walled pipes under external pressure, and the range of experimental pipes' D/t is from 23 to 82. The study of pipeline collapse under the smaller D/t range will be carried out in the fourth section of this paper, using finite element simulation combined with published experimental results. In particular, the full-scale pipeline used in this experiment is consistent with the existing pipeline types, and the experimental results can provide references for engineering construction.

3.1 Test procedure

The general-scale hyperbaric apparatus is shown in Fig. 4 and consists of the main chamber, a hyperbaric sealing system, a hydraulic loading controlling system, and a data acquisition system. This device has a length of 12.0 m and an inner diameter of 2.0 m and can perform multiple sets of pipeline collapse tests simultaneously.

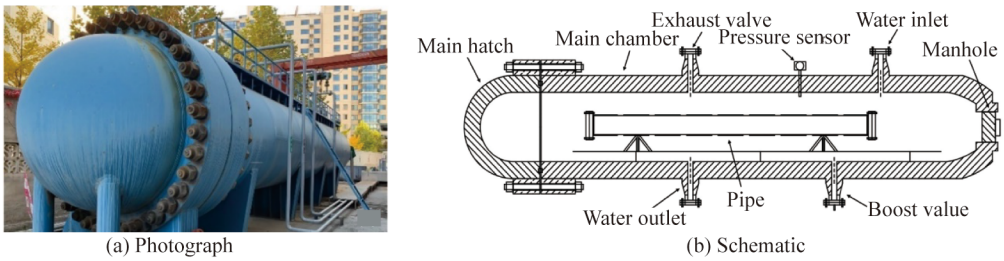

(a) Photograph (b) Schematic

Fig. 4. General-scale hyperbaric apparatus.

The pipes used in the experiment are SS304 stainless steel pipe and Q345 carbon steel pipe, which correspond to the model experiment and full-scale experiment of the pipe respectively. The material properties of the experimental pipe were obtained by uniaxial tensile test on pipe slices, as shown in Table 1.

Before the pressurization experiment, measure the geometric parameters of the pipeline in detail, including the outer diameter D, the average thickness t, and the maximum values of local ovality f_0. The detailed parameters are shown in Table 2. Fig. 5 shows the sealing form at both ends of the pipeline. The high-pressure flange is welded to the end of the pipeline, and the blind plate and the flange are connected by bolts to achieve pipeline sealing.

Table 1 Material properties of the experimental pipe

Material	E	$\sigma_{0.2}$(MPa)	σ_y (MPa)	n
SS304	193000	205	184.5	7.5
Q345	204700	345	299.6	12

Note: $\sigma_{0.2}$ is the yield strength at 0.2% plastic strain.

Put multiple experimental pipes in one pressurization test. The pressure sensor located in the cabin recorded the pressure changes in the cabin during the experiment. As taking the second pressurization test as an example, the change of pressure in the hyperbaric chamber with time is shown in Fig. 6. It can be seen that as the water pressure in the cabin continues to increase, five groups of experimental pipes (R5, R4, R3, F2, R1) are collapsed in sequence, and the pressure drop points are the critical collapse pressure P_{co} of the corresponding pipelines. The pressure drop of the full-scale pipe F2 was so big that a pressure relief and water replenishment step had to be executed during the experiment, and

Table 2 Parameter and collapse pressure of pipe specimens

Number	D (mm)	t (mm)	D/t	f_0 (%)	L (m)	Material	P_{co} (MPa)
F1	325.18	7.080	45.93	0.532	7	Q345	4.20
F2	356.27	9.807	36.33	0.338	7	Q345	8.67
R1	50.09	2.100	23.85	0.865	1	SS304	14.39
R2	101.95	2.910	35.03	0.216	2	SS304	8.55
R3	102.34	2.960	34.58	0.460	2	SS304	7.64
R4	108.24	2.930	36.94	0.426	2	SS304	6.64
R5	89.27	1.998	44.68	0.472	1.6	SS304	3.76
R6	168.36	2.962	56.84	0.607	2	SS304	2.03
R7	133.21	1.998	66.67	0.797	2	SS304	1.21
R8	140.60	1.963	71.62	0.456	2	SS304	1.10
R9	158.70	1.938	81.89	2.428	2	SS304	0.71

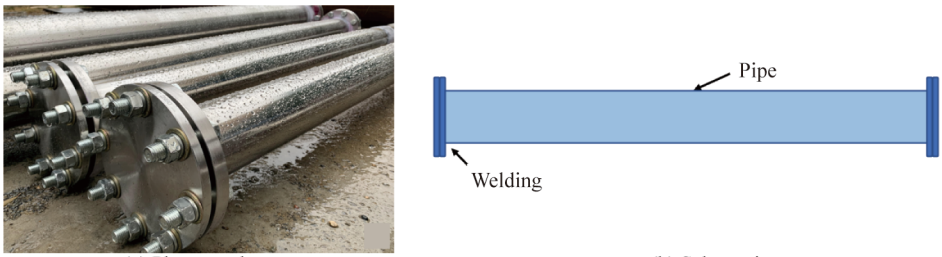

(a) Photograph (b) Schematic

Fig. 5. Experimental pipeline sealing form.

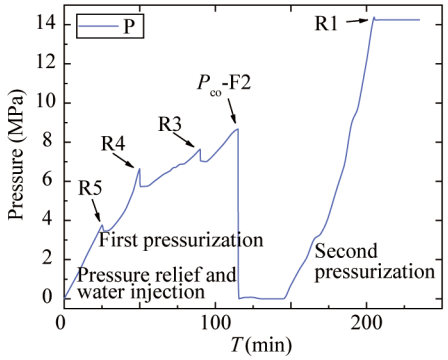

Fig. 6. Variation of pressure in the cabin during the test.

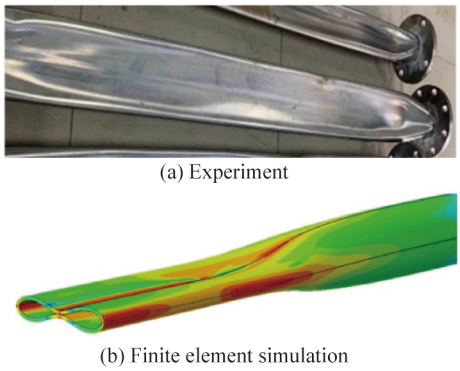

(a) Experiment (b) Finite element simulation

Fig. 7. Pipe buckling trend.

then the second pressurization was performed.

3.2 Experimental results

The detailed parameters and results of the 11 groups of buckling tests are shown in Table 2. Figs. 7 and 8 show the deformation of some test pipes after compression and compare the results of the finite element simulation.

4 Analysis and discussion

4.1 Analysis of experimental results

By observing the test data of R1−R9 in Table 2, D/t of the pipeline increases from 23.85 to 81.89, and the corresponding P_{co} decreases from 14.39 MPa to 0.71 MPa. The changes in these data reflect the relationship between D/t and critical collapse pressure P_{co}. At the same time, by comparing the test results R2 and R3, in the case of a slight decrease in D/t, as the initial ovality f_0 of the pipeline increases, the corresponding P_{co} decreases from 8.55 MPa to 7.64 MPa, which indicates that a larger f_0 will weaken the

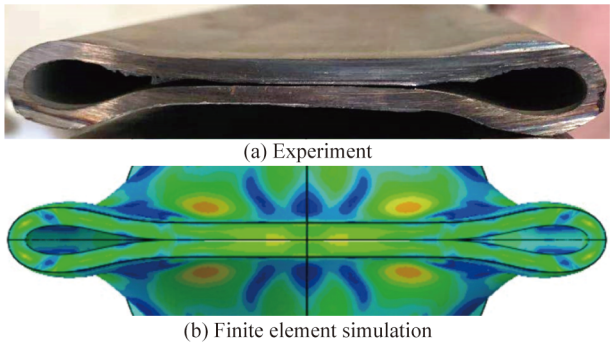

(a) Experiment (b) Finite element simulation

Fig. 8. Collapsed section.

bearing capacity of the pipeline. Through comparing the results of the full-scale pipeline test with the reduced-scale pipeline test, especially F2 and R4, the critical collapse pressure of Q345 steel pipe is significantly higher than that of SS304 stainless steel pipe (8.67 MPa vs. 6.64 MPa) under the conditions of approximate D/t and f_0, which shows that the pipe material also affects the bearing capacity of the pipe to a certain extent. The preliminary analysis of the test results shows that the three factors of the pipeline all affect the critical collapse pressure of the pipeline, namely the diameter-thickness ratio D/t, the ovality f_0 , and the material properties, which are consistent with the DNV specification.

Furthermore, we compared the pipeline collapse pressure results from experiments and numerical calculations. Table 3 compares the experimental results with the corresponding finite element simulation results and the calculation results of the DNV formula (Eq. (2)) and gives the corresponding errors. At the same time, the table also supplements the collapse test results of pipes with smaller diameter-to-thickness ratios given by Sun (2017), which fills up the experimental deficiencies of this research.

Fig. 9 uses D/t as the independent variable to plot the pipeline collapse pressure values from experiments and numerical calculations in Table 3. It can be seen that in the range of D/t>16, both the finite element simulation and the DNV formula have good accuracy, and the average errors are 3.41% and −1.19%, respectively. The new finding is that although D/t of R6, R7, R8, and R9 tests exceed the applicable range of the DNV formula, the results obtained by incorporating the parameters into Eq. (2) are still in good agreement with the experimental results and the finite element simulation results. It shows that the DNV formula based on the ideal elastoplastic hypothesis is still applicable in the range of 45<D/t<80.

Then focus on the test results of D/t<16, it can be found that the calculation results of the DNV formula are significantly smaller than the test results and the finite element simulation results, which verifies the existing research results (Athanasopoulos et al., 2019). The DNV formula is indeed conservative in predicting the collapse pressure of thick-walled pipes. On the contrary, finite element simulation truly reflects the pressure-bearing capacity of thick-walled pipes, even radical. It can be seen that the finite element simulation results in the range of D/t<16 are slightly higher than the corresponding test results, but are closer to the test values than the DNV formula result, and the error is controlled within 14%.

Comparing the results from experiments and numerical calculations within a wide range of D/t, we verified the correctness and applicability of the DNV formula and finite element simulation in different D/t ranges: In the range of 16<D/t<80, both DNV formula and finite element simulation have high accuracy. In the range of D/t<16, as D/t decreases, the calculated value of the DNV formula gradually deviates from the test value, which is expressed as conservative. The finite element simulation results are too large, but the error distribution is within the acceptable range.

4.2 Parameter study

By comparing the results of pipe collapse pressure obtained by experiments and numerical calculations (including DVN specifications and finite element simulation), we found that the main controversy was centered on the collapse of thick-walled pipes. Compared with the experimental value, the classical solution method DNV specification is more conservative in predicting the collapse pressure of thick-walled pipelines, while the finite element simulation result is slightly larger than the experimental value. Based on this, we took the external overpressure failure of thick-walled pipes as the focus of follow-up research and conducted

Table 3 Comparison of experimental and numerical results

Number	D/t	f_0 (%)	E (GPa)	$\sigma_{0.2}$ (MPa)	P_{co}-EXP (MPa)	P_{co}-FEM (MPa)	Error (%)	P_{co}-DNV (MPa)	Error (%)
F1	45.93	0.532	204.7	345	4.20	4.36	3.86	4.234	0.81
F2	36.33	0.338	204.7	345	8.67	8.85	2.15	8.324	−3.94
R1	23.85	0.865	193	205	14.39	14.78	2.75	14.192	−1.34
R2	35.03	0.216	193	205	8.55	8.65	1.23	7.684	−10.07
R3	34.58	0.460	193	205	7.64	7.99	4.65	7.922	3.76
R4	36.94	0.426	193	205	6.64	6.91	4.14	6.749	1.72
R5	44.68	0.472	193	205	3.76	4.10	9.19	4.069	8.36
R6	56.84	0.607	193	205	2.03	2.05	1.23	2.018	−0.34
R7	66.67	0.797	193	205	1.21	1.25	3.73	1.241	2.98
R8	71.62	0.456	193	205	1.10	1.09	−1.18	1.050	−4.78
R9	81.89	2.428	193	205	0.71	0.70	−0.90	0.578	−18.54
H1	12.03	0.44	193	254	47.37	49.08	3.61	33.39	−29.5
H2	12.02	0.52	193	254	43.69	48.33	10.6	33.39	−23.6
H3	12.68	0.94	193	254	39.31	43.39	10.4	30.60	−22.2
H4	12.62	1.1	193	254	37.17	42.38	14.0	30.41	−18.2
S1	16.35	0.514	193	348	38.01	41.12	8.18	39.65	4.33
S2	16.45	0.36	193	348	38.82	40.86	5.26	39.44	1.60

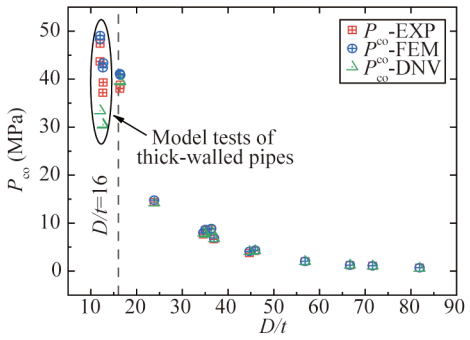

Fig. 9. Comparison of experimental and numerical results of P_{co}.

a systematic parameter study on the critical collapse pressure of thick-walled pipes.

Based on the analysis of experimental results, the critical collapse pressure of the thick-walled pipe is regarded as a function of the pipe diameter-to-thickness ratio D/t, ovality f_0, and material grade $\sigma_{0.2}/E$. At the same time, both sides of the equation are treated as dimensionless, as shown in Eq. (7).

$$\frac{P_{co}}{\sigma_{0.2}} = f\left(\frac{D}{t}, \frac{\sigma_{0.2}}{E}, f_0\right). \tag{7}$$

The selection range of each parameter in the finite element model is shown in Table 4. Use Python scripts to build the finite element models mentioned in Section 2 in batches. After changing the values of different parameters in the finite element model and solving the model, a pipeline collapse simulation database with more than 420 sets of models was established as the basis for subsequent parameter analysis.

Table 4 Parameter range under formula correction

Parameter	Value
D/t	10, 11, 12, 13, 14, 15, 17, 19, 20, 22, 26, 30
f_0 (%)	0.5, 0.75, 1.0, 1.25, 1.5, 2.0, 3.0
$\sigma_{0.2}/E$	0.001316(SS304-1), 0.001653(SS304-2), 0.001685(Q345), 0.0018906(API-X60), 0.00217265(API-X65)

4.2.1 *Pipe diameter-to-thickness ratio D/t*

By taking the API-X65 type pipeline as an example, Fig. 10 shows the relationship between the pipeline collapse pressure and the pipe diameter-thickness ratio D/t. Both finite element simulation and DNV formula calculation results show that the smaller D/t, the larger the corresponding critical collapse pressure. The difference between the two is that when D/t gradually decreases from 20+, the deviation between the DNV calculated value and the finite element result gradually increases, which is the same as the conclusion drawn in the analysis of the experimental results in Section 4.1. The elastic instability pressure P_{el} and the plastic failure pressure P_p of the ideal ring are also plotted in Fig. 10 (from Eqs. (3) and (4)). These two solving equations are based on the ideal elastoplastic assumption of the material, and both jointly determine the value of P_{co}-DNV. It can be seen that, without considering the plastic hardening effect of the material, the calculated value of the plastic failure pressure P_p of the thick-walled pipe is much smaller than the FEM value, which leads to a small P_{co}-DNV.

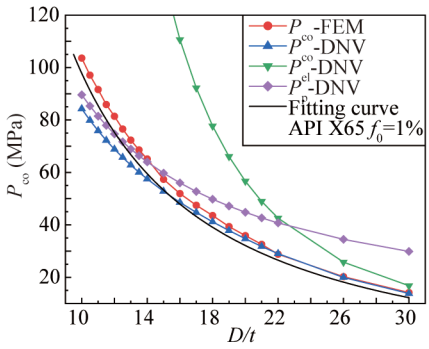

Fig. 10. Relationship between P_{co} and D/t.

The stress cloud diagrams of thick-walled and thin-walled pipes at the moment of collapse in Fig. 11 further illustrate the reason why the DNV formula is conservative in predicting the critical collapse pressure of thick-walled pipes. In the thickness direction of the pipe, the maximum stress of the thick-walled pipe covers most of the pipe wall, indicating that most of the materials have entered the plastic stage, and the buckling of the pipe is manifested as the yield phenomenon of the material. On the contrary, when the thin-walled pipe is buckling, most of the materials are in the elastic stage, and the local buckling of the pipe is manifested as structural instability. The alloy steel commonly used in submarine pipelines will show an obvious plastic hardening effect after entering the yield stage, and this effect is more obvious in thick-walled pipelines. By taking into account the plastic hardening effect mentioned above, the collapse of the thick-walled pipe in the plastic stage can no longer be described by the original yield stress. The neglect of the above phenomenon has led to conservative predictions of the DNV formula.

4.2.2 *Pipe ovality f_0*

Also by taking API-X65 type pipeline as an example, Fig. 12 shows the relationship between collapse pressure and ovality f_0 at different D/t. Whether it is a thick-walled pipe or a thin-walled pipe, the greater the ovality, the lower the collapse pressure. Among them, when the ovality of the pipeline itself increased from 0.5% to 3%, the collapse pressure of the pipeline with D/t=11 dropped by 14.7 MPa, a decrease of 15.5%; and the collapse pressure of the D/t=30 pipeline was reduced by 4.91 MPa, a decrease of 31.4%. The data show that the sensitivity of pipelines' collapse pressure to the ovality f_0 is proportional to the diameter-to-thickness ratio D/t, and the ovality of the pipeline should be strictly controlled for thin-walled pipelines.

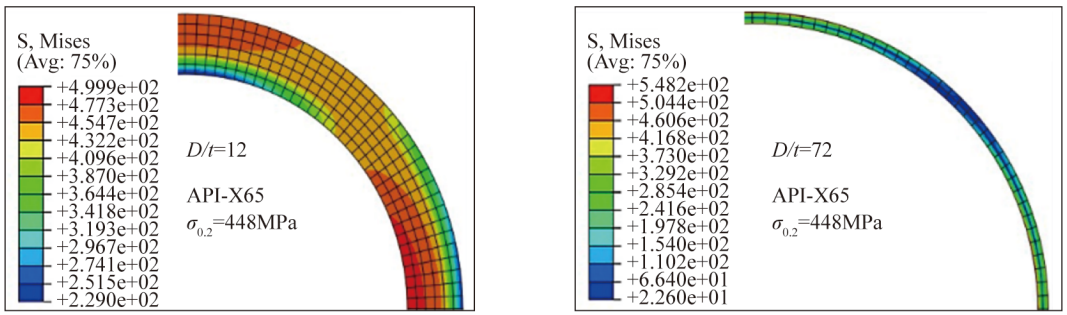

(a) Thick-walled pipe (b) Thin-walled pipe

Fig. 11. Sectional stress cloud diagrams.

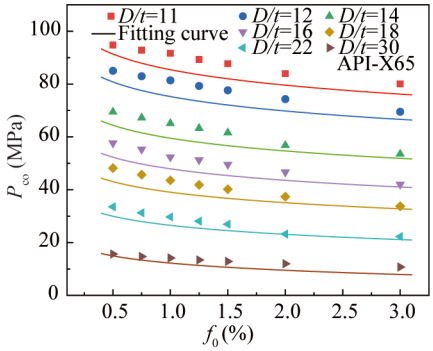

Fig. 12. Relationship between P_{co} and f_0 with different D/t.

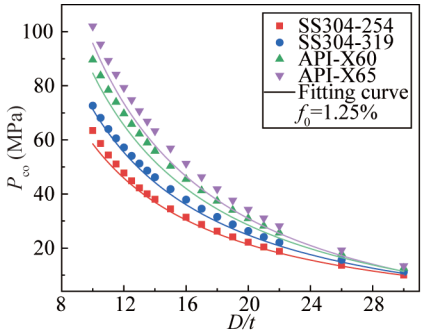

Fig. 14. Relationship between P_{co} and D/t with different pipe material grades.

4.2.3 *Pipe material grade*

Figs. 13 and 14 show the relationship between pipe material grade and collapse pressure from two perspectives respectively. With different D/t, upgrading the grade of pipe material can significantly increase its corresponding collapse pressure. The difference is that the benefits of upgrading steel grades for thick-walled pipes are significantly higher than those for thin-walled pipes. Specifically, when the steel grade was upgraded from SS304 to API-X65, the collapse pressure of the pipeline with D/t=10 increased by 40.4 MPa, an increase of 62.4%. The corresponding collapse pressure of the pipeline with D/t=30 only increased by 3.57 MPa, an increase of 32.0%.

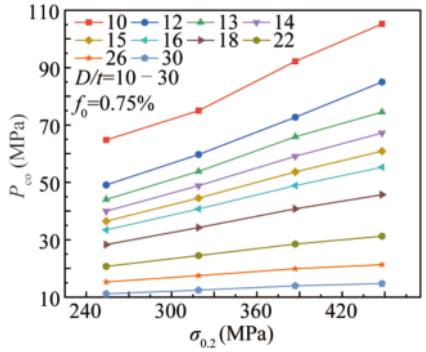

Fig. 13. Relationship between P_{co} and pipe material grade with different D/t.

4.3 Collapse pressure prediction

The final parameter fitting is based on a wide range of finite element simulation results, taking into account the deviation of the finite element simulation and the experimental results, and the buckling characteristics obtained in the parameter analysis. The Levenberg-Marquardt optimization algorithm in the least square method is used to fit the relationship curve between each parameter and the pipeline collapse pressure. The final form of the fitting formula is

$$\frac{P_C}{\sigma_{0.2}} = 4.85\left(\frac{D}{t}\right)^{-0.99}(100f_0)^{-0.04}\left(\frac{\sigma_{0.2}}{E}\right)^{0.05} - 4.46\left(\frac{D}{t}\right)^{-0.39}f_0^{0.04}\left(\frac{\sigma_{0.2}}{E}\right)^{0.38}. \quad (8)$$

The curve corresponding to the above formula is also drawn in Figs. 10, 12 and 14, to show the overall fitting effect. It can be seen that with the changes of pipe diameter-to-thickness ratio D/t, ovality f_0, and material grade $\sigma_{0.2}/E$, the formula results have the same trends as the finite element simulation results, and these changing trends truly reflect the buckling characteristics of thick-walled pipes. At the same time, we comprehensively considered the above deviation between the finite element simulation results and the experimental results, and conservatively fitted the finite element simulation results to further reduce the error with the true value. The main applicable range of Eq. (8) is $10<D/t<16$. We believe that this formula is based on extensive finite element simulation results, and combined with the experi-

mental results of existing research. It can obtain better results when predicting the critical collapse pressure of thick-walled pipelines, and will effectively fill the blank of the DNV formula. After the effective pipeline parameters are given, the corresponding P_{co} can be quickly obtained by substituting Eq. (8), so this formula has certain engineering application significance.

5 Conclusions

Based on the pipeline collapse experiment and finite element simulation, this paper explores the bearing capacity of the pipeline under external pressure in a wide range of diameter-thickness ratios. By conducting the pipeline collapse experiments in the range of $23<D/t<80$ and comparing the experimental results, the applicability and accuracy of the DNV specification and finite element simulation in the corresponding range of D/t have been verified respectively. Moreover, combined with published experimental results and finite element simulations, the conservative prediction of the DNV formula for thick-walled pipelines has been revised. The main conclusions can be drawn.

(1) D/t and f_0 geometrically affect the critical collapse pressure P_{co} of the pipeline. Under the premise of controlling other variables, the smaller D/t and f_0 means the larger corresponding P_{co}, and upgrading the grade of pipe material can always get a larger P_{co}. In terms of sensitivity, compared with thin-walled pipes, the collapse pressure of thick-walled pipes is more sensitive to the grade of pipe material, but the opposite is true for ovality.

(2) For predicting the critical collapse pressure of pipeline in the range of $16<D/t<80$, DNV formula and finite element simulation both have good applicability and correctness, which has been verified theoretically and physically in this paper. For thick-walled pipes ($10<D/t<16$), compared with the test results, the prediction of the critical collapse pressure given by the DNV specification is lower, while the finite element simulation result is slightly higher.

(3) Based on the parameter fitting of the database containing finite element simulation and thick-walled pipeline collapse experiment results, a calculation formula for the critical collapse pressure of pipelines in the range of $10<D/t<16$ is given. This formula can better reflect the buckling characteristics of thick-walled pipelines and give a sufficiently accurate prediction of the critical collapse pressure.

References

American Petroleum Institute, 1999. Design, construction, operation, and maintenance of offshore hydrocarbon pipelines (limit state design), in: *Oil and Gas Pipelines*: *Integrity and Safety Handbook*, third ed., American Petroleum Institute, Washington, DC.

Athanasopoulos, N., Gavalas, E. and Papaefthymiou, S., 2019. Prediction of pipeline collapse due to hydrostatic pressure, *International Journal of Structural Integrity*, 10(1), 55–66.

Bastola, A., Wang, J.K., Mirzaee-Sisan, A. and Njuguna, J., 2014. Predicting hydrostatic collapse of pipes using finite element analysis, *Proceedings of the ASME 2014 33rd International Conference on Ocean*, *Offshore and Arctic Engineering* (*OMAE 2014*), San Francisco, CA.

Corradi, L., Luzzi, L. and Trudi, F., 2005. Plasticity-instability coupling effects on the collapse of thick tubes, *International Journal of Structural Stability and Dynamics*, 5(1), 1–18.

Det Norske Veritas, 2013. *Submarine Pipeline Systems*, DNV-OS-F101, Det Norske Veritas, Oslo.

Det Norske Veritas Lt da, 2014. *Collapse Assessment of Offshore Pipelines with D/t<20- Joint Industry Project Proposal* (DRAFT), Brazil Oil & Gas, Rio de Janeiro, 1–8VI5EU, Rev. 1.

DNVGL, 2017. *Submarine Pipeline Systems*, DNVGL-ST-F101-2017.

Dvorkin, E.N. and Toscano, R.G., 2013. *Finite Element Analysis of the Collapse and Post-Collapse Behavior of Steel Pipes*: *Applications to the Oil Industry*, Springer, Berlin, Heidelberg.

Dyau, J.Y. and Kyriakides, S., 1993. On the localization of collapse in cylindrical shells under external pressure, *International Journal of Solids and Structures*, 30(4), 463–482.

Fallqvist, B., 2009. *Collapse of Thick Deepwater Pipelines due to Hydrostatic Pressure*, MSc. Thesis, Department of Solid Mechanics, Royal Institute of Technology (KTH), Stockholm.

Fan, Z.T., Yu, J.X., Sun, Z.Z. and Wang, H.K., 2017. Effect of axial length parameters of ovality on the collapse pressure of offshore pipelines, *Thin-Walled Structures*, 116, 19–25.

Guarracino, F., Fraldi, M., Freeman, R. and Slater, S., 2011. Hydrostatic collapse of deepwater pipelines, a rigorous analytical approach, *Offshore Technology Conference*, Houston, TX.

Haagsma, S.C. and Schaap, D., 1981. Collapse resistance of submarine lines studied, *Oil and Gas Journal*, 79(2), 86–95.

He, T., Duan, M.L. and An, C, 2014. Prediction of the collapse pressure for thick-walled pipes under external pressure, *Applied Ocean Research*, 47, 199–203.

Hibbitt, H.D., Karlsson, B.I. and Sorensen, P., 2006. *ABAQUS Theory Manual*, Version 6.3, Pawtucket, Rhode Island, USA.

Hibbitt, H.D., Karlsson, B.I. and Sorensen, P., 2014. *ABAQUS*, *Analysis User Guide* Version 6.14, Rhode Island, USA.

Kara, F., Navarro, J. and Allwood, R.L., 2010. Effect of thickness variation on collapse pressure of seamless pipes, *Ocean Engineering*, 37(11-12), 998–1006.

Kyriakides, S. and Babcock, C.D., 1981. Large deflection collapse analysis of an inelastic inextensional ring under external pressure, *International Journal of Solids and Structures*, 17(10), 981–993.

Langner, C.G. and Ayers, R.R., 1985. Feasibility of laying pipelines in deep waters, *Proceedings of the 4th International Offshore Mechanics and Arctic Engineering Symposium*, I, Dallas,TX, 478–489.

Lu, Y., Wang, R.Q., Han, Q.H., Yu, X.L. and Yu, Z.C., 2022. Experimental investigation on the corrosion and corrosion fatigue behavior of butt weld with G20Mn5QT cast steel and Q355D steel under dry-wet cycle, *Engineering Failure Analysis*, 134, 105977.

Mantovano, L., Chebaro, M.R., Ernst, H.A., de Souza, M., Timms, C. and Chad, L.C., 2011. The influence of the UOE-SAWL forming process on the collapse resistance of deepwater linepipe, *Proceedings of the ASME 2011 30th International Conference on Ocean, Offshore and Arctic Engineering* (*OMAE 2011*), Rotterdam.

Murphey, C.E. and Langner, C.G., 1985. Ultimate pipe strength under bending, collapse and fatigue, *Proceedings of the 4th International Conference on Offshore Mechanics and Arctic Engineering,* Vol. I, Dallas, TX, pp. 467–477.

Palmer, A.C. and King, R.A., 2008. *Subsea Pipeline Engineering*, second ed., PennWell, Tulsa, pp. 327–360.

Simo, J.C. and Armero, F., 1992. Geometrically non-linear enhanced strain mixed methods and the method of incompatible modes, *International Journal for Numerical Methods in Engineering*, 33(7), 1413–1449.

Sun, Z.Z., 2017. *On the Buckling Instability Mechanism of Deep-Sea Pipeline*, Ph.D. Thesis, Tianjin University, Tianjin. (in Chinese)

Timoshenko, S.P. and Gere, J.M., 1961. *Theory of Elastic Stability*, second ed., McGraw-Hill, New York.

Yu, J.X., Han, M.X., Duan, J.H., Yu, Y. and Sun, Z.Z., 2019. A modified numerical calculation method of collapse pressure for thick-walled offshore pipelines, *Applied Ocean Research*, 91, 101884.

Zhang, X.H. and Pan, G., 2020. Collapse of thick-walled subsea pipelines with imperfections subjected to external pressure, *Ocean Engineering*, 213, 107705.